Journal of the Mechanics and Physics of Solids 135 (2020) 103805

Contents lists available at ScienceDirect

Journal of the Mechanics and Physics of Solids

journal homepage: www.elsevier.com/locate/jmps

A general expression for linearized properties of swollen elastomers undergoing large deformations

Dai Okumura [a,*], Hironori Kawabata [b], Shawn A. Chester [c]

[a] Department of Mechanical Systems Engineering, Nagoya University, Furo-cho, Chikusa-ku, Nagoya 464-8603, Japan
[b] Department of Micro-Nano Systems Engineering, Nagoya University, Furo-cho, Chikusa-ku, Nagoya 464-8603, Japan
[c] Department of Mechanical Engineering, New Jersey Institute of Technology, Newark, NJ 07102, USA

ARTICLE INFO

Article history:
Received 5 August 2019
Revised 7 October 2019
Accepted 24 November 2019
Available online 27 November 2019

Keywords:
Constitutive behavior
Swelling
Hyperelasticity
Solvent migration
Finite strain

ABSTRACT

In this study, we develop a general expression for the linearized properties of swollen elastomers undergoing large deformations. The free energy function of swollen elastomers is assumed to obey the Frenkel–Flory–Rehner hypothesis, i.e., the elastic and mixing contributions are additive. The elastic strain energy is not assumed to have a particular form but is assumed only to be a function of a set of strain-invariants. A linearization procedure is used to obtain the general expression for the Young's modulus and Poisson's ratio under an arbitrary base state. The derived expression includes a characteristic term, which has the ability to describe a transient state between the extreme states prescribed by two distinct conditions. The verification is performed by estimating the shear modulus and considering the original Flory–Rehner framework. In addition, to show the usefulness, an extended Gent model is examined to elucidate the interactions between limiting chain extensibility and the second strain-invariant.

1. Introduction

The Frenkel–Flory–Rehner (FFR) hypothesis (Frenkel, 1940; Flory and Rehner, 1943) provides a basis for interpreting the mechanical and swelling behavior of swollen elastomers, including polymeric gels such as hydrogels (Flory, 1953; Treloar, 1975; Doi, 2013). The FFR hypothesis assumes that the free energy function of swollen elastomers consists of the sum of two terms associated with polymer stretching (i.e., the elastic strain energy) and the mixing of polymer and solvent molecules (i.e., the mixing energy). In the Flory–Rehner (FR) framework (Flory and Rehner, 1943), the elastic and mixing contributions are derived from the Gaussian network theory (i.e., a Neo–Hookean (NH) model) and the Flory–Huggins solution theory, respectively. The NH model can be replaced by a more sophisticated strain-energy function for rubber elasticity. Chester and Anand (2010, 2011) and Li et al. (2014) introduced the Arruda–Boyce and Gent models, respectively, to the FR framework, to consider the non-Gaussian chain effect, i.e., the effect of limiting chain extensibility (Okumura and Chester, 2018). Further, Okumura et al. (2016, 2018) extended the NH model using two scaling exponents to reproduce two independent effects of swelling on the Young's modulus and the osmotic pressure of the swollen elastomers. There is no doubt that the strain-energy function in the FR framework will become more complex with experimental observations and model refinements (e.g., Davidson and Goulbourne, 2013; Drozdov and Christiansen, 2013; Mao and Anand, 2018).

* Corresponding author.
E-mail address: dai.okumura@mae.nagoya-u.ac.jp (D. Okumura).

https://doi.org/10.1016/j.jmps.2019.103805
0022-5096/

Hong et al. (2009) demonstrated that the FR framework is systematically implemented in commercially available finite element software because the free energy function takes an explicit form as a function of the deformation gradient and the chemical potential of the external solvent. The boundary value problem of swollen elastomers is equivalent to that of a compressible hyperelastic material. The elasticity tensor is calculated from the first and second derivatives of the free energy function with respect to the strain-invariants (Holzapfel, 2000). For example, the finite element package Abaqus provides the user-defined material subroutine UHYPER (Abaqus, 2014) in which only the equations of the derivatives have to be defined (cf. Kang and Huang, 2010a). This subroutine allows researchers to perform finite element analyses of various problems focused on the mechanical and swelling behavior of swollen elastomers (Hong et al., 2009; Liu et al., 2015; Okumura et al., 2014, 2015). Solvent migration in a transient state can also be analyzed by assuming a diffusion model (Hong et al., 2008; Bouklas et al., 2015; Toh et al., 2015). In contrast, if researchers intend to develop and investigate an extended version of the FR framework, they will need to solve the boundary value problem via finite element analysis. However, that is a time consuming procedure that requires special skills. Accordingly, a simple analytical procedure is needed for estimating and understanding the constitutive behavior predicted by such extended model.

The effects of swelling on the Young's modulus E and Poisson's ratio ν of swollen elastomers were analyzed by a linearization procedure (Boyce and Arruda, 2001; Bouklas and Huang, 2012). The NH model predicts $E = E_{\rm d}\, J^{-1/3}$, where $E_{\rm d}$ is the Young's modulus of the dry state and J is the volume swelling ratio. This simple relation is derived when J is preserved so that $\nu = 1/2$. When the change in J is allowed and the chemical potential of the external solvent is preserved, the FR framework with the NH model predicts $\nu = 0.2$–0.5, which depends on a set of material parameters including the Flory–Huggins interaction parameter χ. As χ decreases from 1 to 0 (where good solvents have a low χ), ν decreases from 0.5 to 0.2 (Bouklas and Huang, 2012). This is caused by an increase, or decrease, of the volume swelling ratio under uniaxial tension or compression when the chemical potential is fixed (Flory, 1953; Treloar, 1975), leading to Young's modulus being expressed as $E = (2/3)(1+\nu)\, E_{\rm d}\, J^{-1/3}$. If the NH model is extended by two scaling exponents, ν can also take a negative value (Okumura et al., 2016, 2018). These studies assumed the base state to be stress-free and isotropically swollen (i.e., free swelling). However, other base states are also critical and important for swollen elastomers undergoing large deformations. For instance, when a gel column and a gel film bonded on a rigid substrate or sandwiched between rigid plates are analyzed using nonlinear buckling theories, various base states should be considered (Liu et al., 2011). It is thus worthwhile developing a general expression for the linearized properties of swollen elastomers without prior determination of the strain-energy function and the base state.

In this study, a general expression for the linearized properties of swollen elastomers undergoing large deformations is derived and analyzed. Section 2 presents the fundamental relations obtained from the FR framework. No particular form is considered to be the strain-energy function, which is only assumed only to be a function of a set of strain-invariants. Section 3 reports on a linearization procedure that yields a matrix form of the linearized properties in terms of principal stretches. In Section 4, a general expression of Young's modulus and Poisson's ratio is derived considering various typical base states. The derived expression includes a characteristic term, which has the ability to describe a transient state between the extreme states prescribed by two distinct conditions. The verification is performed by estimating the shear modulus and considering the original FR framework. Section 5 is devoted to showing the usefulness of the derived expression. An extended Gent model is examined as the strain-energy function to elucidate the interactions of limiting chain extensibility and the second strain-invariant. Finally, conclusions are presented in Section 6.

2. Fundamental relations of swollen elastomers

The FFR hypothesis and FR framework (Frenkel, 1940; Flory and Rehner, 1943) assume that to describe the mechanical and swelling behavior of swollen elastomers, the free energy function W is expressed as the sum of the elastic strain energy $W_{\rm e}$ and the mixing energy $W_{\rm m}$, i.e.,

$$W = W_{\rm e}(I_1, I_2, J) + W_{\rm m}(C), \tag{1}$$

where I_1, I_2 and J are strain-invariants and C is the nominal concentration of solvent molecules. The employment of the principal stretches λ_i ($i = =1, 2, 3$) leads to $I_1 = \lambda_1^2 + \lambda_2^2 + \lambda_3^2$, $I_2 = \lambda_1^2\lambda_2^2 + \lambda_2^2\lambda_3^2 + \lambda_3^2\lambda_1^2$ and $J = \lambda_1\lambda_2\lambda_3$. Although the original FR framework was developed based on the specific forms of $W_{\rm e}$ and $W_{\rm m}$ derived from the Gaussian network theory (i.e., the NH model) and the Flory–Huggins solution theory, respectively, the present study considers a different version of $W_{\rm e}$ and assumes that $W_{\rm e}$ is a function of a set of strain-invariants, namely I_1, I_2 and J.

Considering the incompressibility of a network of a polymer and liquid solvent, the volume of swollen elastomers is expressed as the sum of the volume of the dry network and that of the solvent (Flory, 1953; Treloar, 1975; Hong et al., 2009). The volume swelling ratio of the swollen elastomers is equal to J and is expressed as

$$J = 1 + \upsilon C, \tag{2}$$

where υ is the volume per solvent molecule. When a Lagrange multiplier is used in Eq. (1) to impose the constraint of Eq. (2), then

$$W = W_{\rm e}(I_1, I_2, J) + W_{\rm m}(C) + \Pi(1 + \upsilon C - J), \tag{3}$$

where Π is the Lagrange multiplier and is referred to as the osmotic pressure caused by mixing in the present study (Kang and Huang, 2010a; Li et al., 2014).

It is remarked here that in the present study, the principal components are used (i.e., $I_1 = \lambda_1^2 + \lambda_2^2 + \lambda_3^2$, $I_2 = \lambda_1^2\lambda_2^2 + \lambda_2^2\lambda_3^2 + \lambda_3^2\lambda_1^2$ and $J = \lambda_1\lambda_2\lambda_3$) and there is no need to consider shear components using the deformation gradient because the Young's modulus and Poisson's ratio are estimated in a linearization procedure (see Sections 3 and 4). It is also remarked that although the present study considers the molecular incompressibility for simplicity, if the compressibility of the elastomer is introduced in Eqs. (2) and (3), J is separated into elastic and swelling components, J_e and J_s (i.e., $J = J_e J_s$), so that the contribution of J_e should be added as a volumetric term in W_e (Chester and Anand, 2011).

Eq. (3) gives the nominal stress in each direction of the principal stretches ($i = =1, 2, 3$),

$$s_i = \frac{\partial W}{\partial \lambda_i} = 2\lambda_i \frac{\partial W_e}{\partial I_1} + 2\lambda_i (I_1 - \lambda_i^2) \frac{\partial W_e}{\partial I_2} + \frac{J}{\lambda_i}\left(\frac{\partial W_e}{\partial J} - \Pi \right), \text{ no sum on } i, \tag{4}$$

where $\partial I_1/\partial \lambda_i = 2\lambda_i$, $\partial I_2/\partial \lambda_i = 2\lambda_i(I_1 - \lambda_i^2)$ and $\partial J/\partial \lambda_i = J/\lambda_i$. The nominal stress is transformed into the true stress t_i as $t_i = \lambda_i s_i/J$ (no sum on i). When the chemical potential, μ, of the solvent in the swollen elastomer, Eqs. (2) and (3) lead to

$$\mu = \frac{\partial W}{\partial C} = \upsilon \left(\frac{\partial W_m}{\partial J} + \Pi \right). \tag{5}$$

When μ is balanced with the chemical potential of the external solvent, $\mu = 0$ expresses the equilibrium swelling state in practice (Kang and Huang, 2010b; Okumura et al., 2015). In contrast, in the transient state, the gradient of μ drives solvent migration (i.e., causes the changes in J and C). A diffusion model provides an evolution equation for J and C (e.g., Hong et al., 2008; Bouklas et al., 2015; Toh et al., 2015). The evolution equation is used to update the values of J and C so that the value of μ is also estimated from Eq. (5). Because $J = 1$ and $C = 0$ at $\mu = -\infty$, the transient state is prescribed in the range between $-\infty < \mu < 0$.

In addition, Eq. (5) shows that J depends on μ and Π, while Eq. (4) shows that Π depends on the combination of s_i and λ_i. When $s_3 = 0$ is explicitly considered, Eqs. (4) and (5) give a specific relation of Π as follows:

$$\Pi = \frac{\mu}{\upsilon} - \frac{\partial W_m}{\partial J} = \frac{2\lambda_3^2}{J}\left\{ \frac{\partial W_e}{\partial I_1} + \left(I_1 - \lambda_3^2\right) \frac{\partial W_e}{\partial I_2} \right\} + \frac{\partial W_e}{\partial J}, \text{ when } s_3 = 0. \tag{6}$$

In this specific case, since Π is expressed using W_e instead of μ and W_m, and various base states can be prescribed using $s_3 = 0$, Eq. (6) is convenient and will be used in Section 4.5 and Appendix B.

3. Matrix form of the linearized properties

This section is devoted to deriving a matrix form of the linearized properties of swollen elastomers. The matrix form is obtained by linearizing Eqs. (4) and (5). Bouklas and Huang (2012) used this approach to derive the linear elastic properties of swollen elastomers from the original FR framework. They assumed the base state to be stress-free and isotropically swollen (i.e., $s_i = 0$ and $\lambda_i = J^{1/3}$) and no change of the chemical potential from the base state (i.e., $\Delta\mu = 0$). Here $\Delta\mu$ is the small perturbation of the chemical potential from the base state. Okumura et al. (2016) assumed the same base state but the effect of $\Delta J = 0$ as well as $\Delta\mu = 0$ was investigated. Here ΔJ is the small perturbation of the volume swelling ratio (i.e., the third strain-invariant) from the base state. In the present study, these assumptions are not imposed in advance so that a matrix form of the linearized properties is derived from an arbitrary base state. To this end, $\Delta(*)$ is defined as a small perturbation of a variable $(*)$, e.g., Δs_i for s_i and $\Delta\lambda_i$ for λ_i.

The present study focuses on the physical meaning of the two specific conditions, $\Delta J = 0$ and $\Delta\mu = 0$, because the two conditions have the ability to estimate the transient effects cause by solvent migration in the linearization procedure, although a diffusion model describes the transient effects as the resulting value of μ ($-\infty < \mu < 0$) in the base state (Section 2). First, when a very short time is given for the small perturbations, diffusion needs time so that solvent migration is prohibited (i.e., $\Delta J = 0$). The condition, $\Delta J = 0$, predicts the instantaneous response and maintains the volume swelling ratio, J, of the base state. In contrast, when a very sufficient time is given for the small perturbations, solvent migration is allowed to achieve equilibrium swelling (i.e., $\Delta\mu = 0$). The condition, $\Delta\mu = 0$, predicts the equilibrium response and maintains the chemical potential, μ, of the base state. In the linearization procedure (this section and Section 4), the transient effects are simply established by considering a transient state between the extreme states prescribed by the two distinct conditions, $\Delta J = 0$ and $\Delta\mu = 0$, and the physical meaning is very clear.

To derive the matrix form, Eq. (4) is first linearized using small perturbations, i.e.,

$$\begin{aligned} \Delta s_i = {} & 2\Delta\lambda_i \frac{\partial W_e}{\partial I_1} + 2\lambda_i \Delta\left(\frac{\partial W_e}{\partial I_1} \right) + 2\left\{ \Delta\lambda_i (I_1 - 3\lambda_i^2) + \lambda_i \Delta I_1 \right\} \frac{\partial W_e}{\partial I_2} \\ & + 2\lambda_i (I_1 - \lambda_i^2) \Delta\left(\frac{\partial W_e}{\partial I_2} \right) + \left(\frac{\Delta J}{\lambda_i} - \frac{J\Delta\lambda_i}{\lambda_i^2} \right) \left(\frac{\partial W_e}{\partial J} - \Pi \right) + \frac{J}{\lambda_i} \left\{ \Delta\left(\frac{\partial W_e}{\partial J} \right) - \Delta\Pi \right\}, \end{aligned} \tag{7}$$

where

$$\begin{cases} \Delta\left(\dfrac{\partial W_\mathrm{e}}{\partial I_1}\right) = \dfrac{\partial^2 W_\mathrm{e}}{\partial I_1^2}\Delta I_1 + \dfrac{\partial^2 W_\mathrm{e}}{\partial I_1 \partial I_2}\Delta I_2 + \dfrac{\partial^2 W_\mathrm{e}}{\partial J \partial I_1}\Delta J \\ \Delta\left(\dfrac{\partial W_\mathrm{e}}{\partial I_2}\right) = \dfrac{\partial^2 W_\mathrm{e}}{\partial I_1 \partial I_2}\Delta I_1 + \dfrac{\partial^2 W_\mathrm{e}}{\partial I_2^2}\Delta I_2 + \dfrac{\partial^2 W_\mathrm{e}}{\partial I_2 \partial J}\Delta J \\ \Delta\left(\dfrac{\partial W_\mathrm{e}}{\partial J}\right) = \dfrac{\partial^2 W_\mathrm{e}}{\partial J \partial I_1}\Delta I_1 + \dfrac{\partial^2 W_\mathrm{e}}{\partial I_2 \partial J}\Delta I_2 + \dfrac{\partial^2 W_\mathrm{e}}{\partial J^2}\Delta J \end{cases}, \tag{8}$$

$$\begin{cases} \Delta I_1 = 2(\lambda_1 \Delta\lambda_1 + \lambda_2 \Delta\lambda_2 + \lambda_3 \Delta\lambda_3) \\ \Delta I_2 = 2\left\{(I_1 - \lambda_1^2)\lambda_1 \Delta\lambda_1 + (I_1 - \lambda_2^2)\lambda_2 \Delta\lambda_2 + (I_1 - \lambda_3^2)\lambda_3 \Delta\lambda_3\right\} \\ \Delta J = J(\Delta\lambda_1/\lambda_1 + \Delta\lambda_2/\lambda_2 + \Delta\lambda_3/\lambda_3) \end{cases}. \tag{9}$$

Eq. (5) is also linearized and gives

$$\Delta\Pi = \frac{\Delta\mu}{\upsilon} - \frac{\partial^2 W_\mathrm{m}}{\partial J^2}\Delta J. \tag{10}$$

Eqs. (8)–(10) allow Δs_i in Eq. (7) to be expressed as a linear function of $\Delta\lambda_i$ and $\Delta\mu$ because λ_i and μ are the known values at an arbitrary base state that is prescribed using Eqs. (4) and (5) (not a specific base state). Eqs. (7) and (10) are the linearized relations between Δs_i, $\Delta\mu$, $\Delta\Pi$ and $\Delta\lambda_i$.

When the small perturbations of the strain and stress in the principal directions are defined as

$$\Delta\varepsilon_i = \frac{\Delta\lambda_i}{\lambda_i}, \text{ no sum on } i, \tag{11}$$

$$\Delta\sigma_i = \frac{\lambda_i \Delta s_i}{J}, \text{ no sum on } i, \tag{12}$$

a matrix form of the linearized properties is consequently given as

$$\begin{Bmatrix} \Delta\sigma_1 \\ \Delta\sigma_2 \\ \Delta\sigma_3 \end{Bmatrix} = \begin{bmatrix} S_{11} + D_1 & S_{12} & S_{31} \\ & S_{22} + D_2 & S_{23} \\ \text{sym.} & & S_{33} + D_3 \end{bmatrix} \begin{Bmatrix} \Delta\varepsilon_1 \\ \Delta\varepsilon_2 \\ \Delta\varepsilon_3 \end{Bmatrix} - \frac{\Delta\mu}{\upsilon}\begin{Bmatrix} 1 \\ 1 \\ 1 \end{Bmatrix}. \tag{13}$$

The components of S_{ij} and D_i are derived and shown in Appendix A. The 3×3 matrix of S_{ij} also has a different expression decomposed into 6 components, namely

$$S_{ij} = \sum_{n=1}^{6} k^{(n)} S_{ij}^{(n)}, \tag{14}$$

where $k^{(n)}$ (n = 1, 2, 3,..., 6) are scalar values that consist of derivatives of W_e and W_m with respect to I_1, I_2 and J, i.e.,

$$k^{(1)} = \frac{4}{J}\left(\frac{\partial W_\mathrm{e}}{\partial I_2} + \frac{\partial^2 W_\mathrm{e}}{\partial I_1^2}\right), \tag{15}$$

$$k^{(2)} = \frac{4}{J}\frac{\partial^2 W_\mathrm{e}}{\partial I_1 \partial I_2}, \tag{16}$$

$$k^{(3)} = \frac{4}{J}\frac{\partial^2 W_\mathrm{e}}{\partial I_2^2}, \tag{17}$$

$$k^{(4)} = 2\frac{\partial^2 W_\mathrm{e}}{\partial I_1 \partial J}, \tag{18}$$

$$k^{(5)} = 2\frac{\partial^2 W_\mathrm{e}}{\partial I_2 \partial J}, \tag{19}$$

$$k^{(6)} = J\left(\frac{\partial^2 W_\mathrm{e}}{\partial J^2} + \frac{\partial^2 W_\mathrm{m}}{\partial J^2}\right) + \frac{\partial W_\mathrm{e}}{\partial J} - \Pi, \tag{20}$$

while $S_{ij}^{(n)}$ (n = 1, 2, 3,..., 6) are the 3×3 matrices that are formed as combinations of λ_i, i.e.,

$$S_{ij}^{(1)} = \lambda_i^2 \lambda_j^2 = S_{ji}^{(1)}, \tag{21}$$

$$S_{ij}^{(2)} = \lambda_i^2 \lambda_j^2 \left\{(I_1 - \lambda_i^2) + (I_1 - \lambda_j^2)\right\} = S_{ji}^{(2)}, \tag{22}$$

$$S_{ij}^{(3)} = \lambda_i^2 \lambda_j^2 (I_1 - \lambda_i^2)(I_1 - \lambda_j^2) = S_{ji}^{(3)}, \tag{23}$$

$$S_{ij}^{(4)} = \lambda_i^2 + \lambda_j^2 = S_{ji}^{(4)}, \tag{24}$$

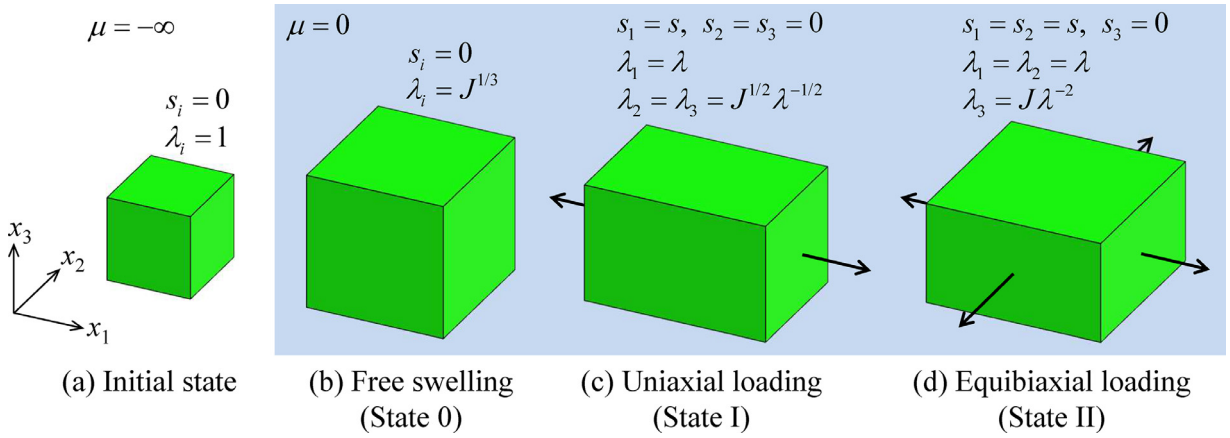

Fig. 1. Schematic illustrations of typical base states; (a) the initial, undeformed dry state, (b) equilibrium free swelling (State 0), (c) equilibrium swelling under uniaxial loading (State I) and (d) equilibrium swelling under equibiaxial loading (State II). For the individual base states, the relations for s, λ and J are obtained from Eqs. (4) and (5). The present study just considers $\mu = 0$ for simplicity, but a specific negative value of μ ($\mu < 0$) can also be used for the base states.

$$S_{ij}^{(5)} = \lambda_i^2(I_1 - \lambda_i^2) + \lambda_j^2(I_1 - \lambda_j^2) = S_{ji}^{(5)}, \tag{25}$$

$$S_{ij}^{(6)} = 1 = S_{ji}^{(6)}. \tag{26}$$

In addition, D_i is rewritten as (Appendix A)

$$D_i = \frac{2\lambda_i^2}{J}\left\{\frac{\partial W_e}{\partial I_1} + (I_1 - 3\lambda_i^2)\frac{\partial W_e}{\partial I_2}\right\} - \frac{\partial W_e}{\partial J} + \Pi. \tag{27}$$

Eqs. (21)–(26) indicate that $S_{ij}^{(n)}$ are symmetric matrices so that S_{ij} is also symmetric because of Eq. (14). It is noted that if the small perturbation of the nominal or true stress, Δs_i or Δt_i, is used instead of $\Delta\sigma_i$ to assemble Eq. (13), the resulting matrix of S_{ij} can be asymmetric depending on the base state. The employment of Eq. (12) maintains the symmetry of S_{ij} at an arbitrary base state. In addition, Eqs. (9) and (11) give

$$\Delta J = J(\Delta\varepsilon_1 + \Delta\varepsilon_2 + \Delta\varepsilon_3), \tag{28}$$

which can be used to rewrite the second term of the right hand side of Eq. (13), leading to

$$\begin{Bmatrix}\Delta\sigma_1\\ \Delta\sigma_2\\ \Delta\sigma_3\end{Bmatrix} = \begin{bmatrix} S_{11} + D_1 - \frac{J\Delta\mu}{\upsilon\Delta J} & S_{12} - \frac{J\Delta\mu}{\upsilon\Delta J} & S_{31} - \frac{J\Delta\mu}{\upsilon\Delta J} \\ & S_{22} + D_2 - \frac{J\Delta\mu}{\upsilon\Delta J} & S_{23} - \frac{J\Delta\mu}{\upsilon\Delta J} \\ \text{sym.} & & S_{33} + D_3 - \frac{J\Delta\mu}{\upsilon\Delta J} \end{bmatrix} \begin{Bmatrix}\Delta\varepsilon_1\\ \Delta\varepsilon_2\\ \Delta\varepsilon_3\end{Bmatrix}. \tag{29}$$

Eqs. (13) and (29) show that the matrix connecting $\Delta\sigma_i$ and $\Delta\varepsilon_i$ is symmetric regardless of the existence of ΔJ and $\Delta\mu$. This ensures that the Young's moduli and Poisson's ratios, which will be derived in Section 4, obey the reciprocal relations (e.g., Vannucci, 2018).

It is incidentally noted that $\Delta J = 0$ and $\Delta\mu = 0$ may be regarded as undrained and drained conditions in the poroelasticity literature, but they are not identically the same because of the fundamental relations (see Section 2). Thus, those expressions are not used in the present study.

4. General expression for Young's modulus and Poisson's ratio

Although Eq. (13) provides the three Young's moduli for loading in the three principal directions and the three distinct Poisson's ratios (owing to the reciprocal relations), the present study does not focus on deriving the whole set of them (Vannucci, 2018) but focuses on considering the effects of solvent migration and base states.

Section 4.1 is devoted to the definition of the Young's modulus and Poisson's ratio, which are derived from Eq. (13) and depend on the two distinct conditions ($\Delta J = 0$ and $\Delta\mu = 0$). Sections 4.2 and 4.4 show the explicit expressions by considering three typical base states (Fig. 1), which are referred to as State 0 (equilibrium free swelling), State I (equilibrium swelling under uniaxial loading) and State II (equilibrium swelling under equibiaxial loading). Here, a specific negative value of μ ($\mu < 0$) can also be used for the base states. However, to avoid confusion, the value of μ is just fixed as $\mu = 0$ and the effects caused by $\Delta J = 0$ and $\Delta\mu = 0$ are in particular investigated here. In Section 4.3, the shear modulus for State 0 is also estimated using Eq. (13). In Section 4.5, the derived expressions are verified by considering the original FR framework.

4.1. Definition of Young's modulus and Poisson's ratio

For uniaxial loading by the principal stress $\Delta\sigma_1$, the Young's modulus, E_1, and Poisson's ratios, ν_{21} and ν_{31}, are defined as

$$\begin{cases} \Delta\sigma_2 = \Delta\sigma_3 = 0 \\ E_1 = \frac{\Delta\sigma_1}{\Delta\varepsilon_1},\ \nu_{21} = -\frac{\Delta\varepsilon_2}{\Delta\varepsilon_1},\ \nu_{31} = -\frac{\Delta\varepsilon_3}{\Delta\varepsilon_1} \end{cases}, \tag{30}$$

Eq. (30) indicates that uniaxial loading is given to the small perturbations, $\Delta\sigma_i$ and $\Delta\varepsilon_i$ (not s_i and λ_i). It is thus noted that ν_{21} and ν_{31} should be distinct from the Poisson function calculated from λ_i (see the definition in Beatty and Stalnaker (1986)). Eq. (30) transforms Eq. (13) into

$$\begin{bmatrix} 1 & S_{12} & S_{31} \\ 0 & S_{22}+D_2 & S_{23} \\ 0 & S_{23} & S_{33}+D_3 \end{bmatrix} \begin{Bmatrix} E_1 \\ \nu_{21} \\ \nu_{31} \end{Bmatrix} = \begin{Bmatrix} S_{11}+D_1 \\ S_{12} \\ S_{31} \end{Bmatrix} - \frac{\Delta\mu}{\upsilon\Delta\varepsilon_1} \begin{Bmatrix} 1 \\ 1 \\ 1 \end{Bmatrix}. \tag{31}$$

Since the base state is prescribed by s_i, λ_i and μ, S_{ij} and D_i are known so that Eq. (31) can be solved with an unknown term of $\Delta\mu/(\upsilon\Delta\varepsilon_1)$.

In Eq. (31), the effects caused by the base state are included in S_{ij} and D_i (see Sections 4.2 and 4.4), while $\Delta\mu/(\upsilon\Delta\varepsilon_1)$ is considered to take a specific value related with an transient state between the extreme states described by the two distinct conditions for the small perturbations (see Section 3), i.e.,

$$\begin{cases} \Delta\mu = 0 \\ \Delta J = 0 \ \leftrightarrow\ 1-\nu_{21}-\nu_{31} = 0 \end{cases}, \tag{32}$$

where $\Delta\mu = 0$ (i.e., $\Delta\mu/(\upsilon\Delta\varepsilon_1) = 0$) is the condition that solvent migration is allowed ($\Delta J \neq 0$) to maintain the chemical potential, μ, of the base state, while $\Delta J = 0$ is the condition that solvent migration is prohibited to maintain the volume swelling ratio, J, of the base state. Here, $1-\nu_{21}-\nu_{31} = 0$ is obtained from Eqs. (28) and (30). Eqs. (7) and (10) imply that when $\Delta J = 0$, $\Delta\mu$ can take on a specific non-zero value ($\Delta\mu \neq 0$). This indicates that the value of $\Delta\mu$ (i.e., $\Delta\mu/(\upsilon\Delta\varepsilon_1)$) describes a transient state and can take on a value in a range between 0 and the specific value related to $\Delta J = 0$ (Sections 4.2 and 4.4). The swelling effects are established by considering the two distinct conditions of Eq. (32).

In fact, swollen elastomers need sufficient time to reach $\Delta\mu = 0$ because the change in $\Delta\mu$ can also be assumed to obey a diffusion model (Hong et al., 2008; Bouklas et al., 2015; Toh et al., 2015). Thus, $\Delta\mu$ is estimated as a result of the time-dependent behavior of solvent migration in swollen elastomers, while $\Delta\varepsilon_1$ can also be time-dependent if the elastomers are assumed to be viscoelastic. The variation in the term of $\Delta\mu/(\upsilon\Delta\varepsilon_1)$ is found to be determined by the ratio of the two different time-dependent behaviors. However, the present study does not directly consider these time-dependent behaviors and just evaluates the swelling effects using the two distinct conditions given in Eq. (32).

4.2. Explicit expressions for State 0

For State 0 (Fig. 1b), the base state of equilibrium free swelling is expressed as

$$s_1 = s_2 = s_3 = 0,\ \lambda_1 = \lambda_2 = \lambda_3 = J^{1/3},\ \mu = 0,\ \text{State 0}, \tag{33}$$

which falls into the base state proposed by Bouklas and Huang (2012); they assumed the base state to be stress-free ($s_i = 0$) and isotropically swollen ($\lambda_i = J^{1/3}$), i.e., free swelling with a non-zero value of μ. Eq. (33) is regarded as the most standard base state since this state is commonly adopted in experimental measurements (McKenna et al., 1989; Bitoh et al., 2011).

Substituting Eq. (33) into Eqs. (21)–(27), it is found that all the components in S_{ij} and D_i take identical values, i.e.,

$$\begin{cases} S_{ij} = S_0 \quad (i = 1,2,3,\ j = 1,2,3) \\ D_i = D_0 \quad (i = 1,2,3) \end{cases}, \text{ for State 0}. \tag{34}$$

From Eqs. (31) and (34), the Young's modulus, E_0 ($= E_1$ for State 0) and the Poisson's ratio, ν_0 ($=\nu_{21} = \nu_{31}$ for State 0), are derived as follows

$$\begin{cases} \nu_0 = \frac{S_0 - \frac{\Delta\mu}{\upsilon\Delta\varepsilon_1}}{D_0+2S_0} \\ E_0 = D_0(1+\nu_0) \end{cases}, \text{ for State 0}. \tag{35}$$

The two conditions of Eq. (32), $\Delta\mu = 0$ and $\Delta J = 0$, which estimate the effects caused by solvent migration, provide

$$\nu_0 = \begin{cases} \frac{S_0}{D_0+2S_0} = \frac{1}{2}\left(1-\frac{D_0}{D_0+2S_0}\right), & \text{with } \Delta\mu = 0 \\ \frac{1}{2}, \quad \text{with } \Delta J = 0 \quad \rightarrow & \frac{\Delta\mu}{\upsilon\Delta\varepsilon_1} = \frac{-D_0}{2} \end{cases}, \text{ for State 0}. \tag{36}$$

It is thus found that E_0 and ν_0 have very simple expressions consisting of S_0 and D_0 ($D_0 > 0$), and that $\Delta\mu$ in a transient state caused by solvent migration can take on a value in the range from $-(D_0/2)\upsilon\Delta\varepsilon_1$ to 0 under tension ($\Delta\varepsilon_1 > 0$) or from 0 to $-(D_0/2)\upsilon\Delta\varepsilon_1$ under compression ($\Delta\varepsilon_1 < 0$). It is further found that the transient effects on E_0 are introduced only via ν_0 (Eq. (35)).

4.3. Estimation of shear modulus

In this subsection, pure shear is considered to estimate the shear modulus of swollen elastomers. When $\Delta\sigma_1 = -\Delta\sigma_2 = \Delta\sigma_{\rm ps}$ and $\Delta\varepsilon_1 = -\Delta\varepsilon_2 = \Delta\varepsilon_{\rm ps}$ are considered as pure shear, Eq. (13) is rewritten as

$$\begin{Bmatrix} \Delta\sigma_{\rm ps} \\ -\Delta\sigma_{\rm ps} \\ 0 \end{Bmatrix} = \begin{bmatrix} S_0+D_0 & S_0 & S_0 \\ & S_0+D_0 & S_0 \\ \text{sym.} & & S_0+D_0 \end{bmatrix} \begin{Bmatrix} \Delta\varepsilon_{\rm ps} \\ -\Delta\varepsilon_{\rm ps} \\ \Delta\varepsilon_3 \end{Bmatrix} - \frac{\Delta\mu}{\upsilon} \begin{Bmatrix} 1 \\ 1 \\ 1 \end{Bmatrix}. \tag{37}$$

It is noted here that to simplify discussion, State 0 (equilibrium free swelling) is just used as the base state (i.e., Eq. (34)). Eq. (37) gives

$$\Delta\varepsilon_3 = \frac{1}{S_0+D_0}\frac{\Delta\mu}{\upsilon} = \frac{1}{S_0}\frac{\Delta\mu}{\upsilon}, \tag{38}$$

where S_0 and D_0 are commonly non-zero values so that this identical equation (Eq. (38)) results in $\Delta\mu = 0$. Further. $\Delta J = 0$ is derived from Eq. (28) because of $\Delta\varepsilon_3 = 0$. It is thus found that pure shear needs both of $\Delta\mu = 0$ and $\Delta J = 0$ (not $\Delta\mu = 0$ or $\Delta J = 0$ as the two distinct states). Consequently, when the shear modulus is defined as $G_0 = \Delta\sigma_{\rm ps}/(2\Delta\varepsilon_{\rm ps})$, Eq. (37) gives

$$G_0 = \frac{\Delta\sigma_{\rm ps}}{2\Delta\varepsilon_{\rm ps}} = \frac{D_0}{2}. \tag{39}$$

This means that the shear modulus does not depend on the swelling process because $\Delta J = 0$ needs no solvent migration and the combination of $\Delta\sigma_1 = -\Delta\sigma_2 = \Delta\sigma_{\rm ps}$ leads to no change in $\Delta\mu$ in total (i.e., $\Delta\mu = 0$).

When D_0 is eliminated using E_0 and ν_0 (i.e., using Eq. (35)), a very popular relation is obtained as

$$G_0 = \frac{E_0}{2(1+\nu_0)}. \tag{40}$$

Eq. (40) is identical with the relation for isotropic linear elasticity. Eq. (40) was first confirmed by Bouklas and Huang (2012). However, their verification was restricted to using both of the original FR framework and a specific condition of $\Delta\mu = 0$. In contrast, the present study demonstrated that Eq. (40) is always established for State 0 regardless of considering $\Delta\mu = 0$ or $\Delta J = 0$ as well as regardless of the particular form of the strain-energy function.

4.4. Explicit expressions for States I and II

In the same way with State 0 (Section 4.2), the different base states (States I and II) are used to derive the corresponding Young's moduli and Poisson's ratios. State I (Fig. 1c), the base state of equilibrium swelling under uniaxial loading, is expressed as

$$s_1 = s,\ s_2 = s_3 = 0,\ \lambda_1 = \lambda,\ \lambda_2 = \lambda_3 = J^{1/2}\lambda^{-1/2},\ \mu = 0,\ \text{State I}, \tag{41}$$

where the directions of $\Delta\sigma_1$ and s_1 are identical. By substituting Eq. (41) into Eqs. (21)–(27), S_{ij} and D_i are found to have the following relations for State I:

$$\begin{cases} S_{11} = S_{\rm Ia} \\ S_{22} = S_{33} = S_{23} = S_{\rm Ib} \\ S_{12} = S_{31} = S_{\rm Ic} \\ D_1 = D_{\rm Ia} \\ D_2 = D_3 = D_{\rm Ib} \end{cases}, \text{for State I}. \tag{42}$$

The Young's modulus, $E_{\rm I}$ ($= E_1$ for State I), and the Poisson's ratio, $\nu_{\rm I}$ ($=\nu_{21} = \nu_{31}$ for State I), are derived from Eqs. (31) and (42), and are expressed in terms of $S_{\rm Ia}$, $S_{\rm Ib}$, $S_{\rm Ic}$, $D_{\rm Ia}$ and $D_{\rm Ib}$ as follows:

$$\begin{cases} \nu_{\rm I} = \dfrac{S_{\rm Ic} - \frac{\Delta\mu}{\upsilon\Delta\varepsilon_1}}{D_{\rm Ib} + 2S_{\rm Ib}} \\ E_{\rm I} = D_{\rm Ia} + D_{\rm Ib}\nu_{\rm I} + S_{\rm Ia} - S_{\rm Ib} + (S_{\rm Ib} - S_{\rm Ic})(1+2\nu_{\rm I}) \end{cases}, \text{for State I}. \tag{43}$$

The two conditions of Eq. (32), $\Delta\mu = 0$ and $\Delta J = 0$, provide

$$\nu_{\rm I} = \begin{cases} \dfrac{S_{\rm Ic}}{D_{\rm Ib}+2S_{\rm Ib}} = \dfrac{1}{2}\left(1 - \dfrac{D_{\rm Ib}+2S_{\rm Ib}-2S_{\rm Ic}}{D_{\rm Ib}+2S_{\rm Ib}}\right), & \text{with } \Delta\mu = 0 \\ \dfrac{1}{2}, \quad \text{with } \Delta J = 0 \quad \rightarrow \quad \dfrac{\Delta\mu}{\upsilon\Delta\varepsilon_1} = \dfrac{-D_{\rm Ib}}{2} - S_{\rm Ib} + S_{\rm Ic} \end{cases}, \text{for StateI}. \tag{44}$$

It is worthwhile to show that when $\lambda = J^{1/3}$ and $s = 0$ in Eq. (41), the base state for State I is reduced to that for State 0 Eq. (33)). This reduction gives $S_{\rm Ia} = S_{\rm Ib} = S_{\rm Ic} = S_0$ and $D_{\rm Ia} = D_{\rm Ib} = D_0$, so that $E_{\rm I}$ and $\nu_{\rm I}$ for State I (Eqs. (43) and ((44)) are properly reduced to E_0 and ν_0 for State 0 Eqs. (35) and (36), respectively. This implies that when $\Delta\mu$ is in a transient state,

it can take a value in the range from $(-D_{\rm lb}/2 - S_{\rm lb} + S_{\rm lc})\upsilon\Delta\varepsilon_1$ to 0 if $\Delta\varepsilon_1 > 0$ or from 0 to $(-D_{\rm lb}/2 - S_{\rm lb} + S_{\rm lc})\upsilon\Delta\varepsilon_1$ if $\Delta\varepsilon_1 < 0$. Additionally, State I can also express a different base state as well as equilibrium swelling under uniaxial loading. For instance, when the value of λ in Eq. (41) is fixed as a constant, the reduced base state expresses equilibrium swelling of an elastomer film sandwiched between rigid plates. Eqs. (43) and (44) are available if the base state to be considered falls into State I.

Finally, for State II (Fig. 1d), the following base state is considered,

$$s_1 = s_2 = s,\ s_3 = 0,\ \lambda_1 = \lambda_2 = \lambda,\ \lambda_3 = J\lambda^{-2},\ \mu = 0,\ \text{State II}, \tag{45}$$

which expresses equilibrium swelling under equibiaxial loading. Further, if λ is fixed as a constant, the reduced base state expresses equilibrium swelling of an elastomer film bonded onto a rigid substrate. Eq. (45) gives the relations of S_{ij} and D_i as

$$\begin{cases} S_{11} = S_{22} = S_{12} = S_{\rm IIa} \\ S_{33} = S_{\rm IIb} \\ S_{23} = S_{31} = S_{\rm IIc} \\ D_1 = D_2 = D_{\rm IIa} \\ D_3 = D_{\rm IIb} \end{cases}, \text{ for State II}. \tag{46}$$

If Eq. (46) is substituted into Eq. (31), the explicit relations can be obtained for the Young's modulus, $E_{\rm II}$ ($=E_1$ for State II), and the two distinct Poisson's ratios, $\nu_{\rm II2}$ and $\nu_{\rm II3}$ ($=\nu_{21}$ and $=\nu_{31}$ for State II, respectively). The derived relations become more complex than those for States 0 and I Eqs. (35) and ((36) for State 0 and Eqs. (43) and (44) for State I). In fact, as the most general state, Eq. (31) can be directly estimated without reductions such as States 0, I and II (ref. anisotropic elasticity, see Vannucci (2018)). The equations are not explicitly shown here although they can be calculated in a similar way as for the analysis of States 0 and I. From now on, we use States 0 and I to focus on demonstrating the usefulness of the derived general expression and to study the effects of solvent migration and the base state on the Young's modulus and Poisson's ratio of swollen elastomers (see Section 5).

4.5. Verification using the original FR framework

It is shown here that if the free energy function consists of simple forms of $W_{\rm e}$ and $W_{\rm m}$, explicit relations for the Young's modulus and Poisson's ratio are obtained from the general expressions derived in Sections 4.2–4.4. The original FR framework (Flory and Rehner, 1943) is employed to determine the forms of $W_{\rm e}$ and $W_{\rm m}$, i.e.,

$$W_{\rm e} = \frac{E_{\rm ref}}{6}(I_1 - 3 - 2\log J),\ \text{the NH model}, \tag{47}$$

$$W_{\rm m} = -\frac{kT}{\upsilon}\left\{\upsilon C\log\left(1 + \frac{1}{\upsilon C}\right) + \frac{\chi}{1+\upsilon C}\right\}, \tag{48}$$

which are derived from the Gaussian network theory and the Flory–Huggins solution theory, respectively. Here, $E_{\rm ref}$ is the reference Young's modulus of the elastomers and χ is the Flory–Huggins interaction parameter. For the NH model, $E_{\rm ref}$ is simply regarded as the Young's modulus of the undeformed, unswollen state at $\lambda_1 = \lambda_2 = \lambda_3 = 1$.

Eq. (47) shows that the NH model includes terms that are independent with respect to I_1 and J. Most of the derivatives of $W_{\rm e}$ become zero, leading to $k^{(1)} = k^{(2)} = k^{(3)} = k^{(4)} = k^{(5)} = 0$ and $k^{(6)} \neq 0$ for Eqs. (15)–(20). It is found that S_{ij} and D_i Eqs. (14) and (27) have remarkably simple relations, i.e.,

$$\begin{cases} S_{ij} = \frac{E_{\rm ref}}{3J}\left\{1 - \lambda_3^2 + \frac{3kT}{E_{\rm ref}\upsilon}\left(\frac{1}{J-1} - \frac{2\chi}{J}\right)\right\} & (i=1,2,3, j=1,2,3) \\ D_i = \frac{E_{\rm ref}}{3J}(\lambda_i^2 + \lambda_3^2) & (i=1,2,3) \end{cases}, \tag{49}$$

To derive Eqs. (49), (6) can be used to replace Π with terms based on $W_{\rm e}$ because Eq. (6) is available in the case of $s_3 = 0$, i.e., for States 0, I and II.

When equilibrium free swelling is considered to be State 0, Eqs. (35), (36) and (40) give the explicit expressions using Eq. (49), i.e.,

$$\nu_0 = \begin{cases} \frac{1}{2} - \frac{J^{2/3}}{2}\left\{1 + \frac{3kT}{E_{\rm ref}\upsilon}\left(\frac{1}{J-1} - \frac{2\chi}{J}\right)\right\}^{-1}, & \text{with } \Delta\mu = 0 \\ \frac{1}{2}, \quad \text{with } \Delta J = 0 \quad \rightarrow \quad \frac{\Delta\mu}{\upsilon\Delta\varepsilon_1} = -\frac{1}{3}E_{\rm ref}J^{-1/3} \end{cases}, \text{ for State 0}, \tag{50}$$

$$E_0 = \frac{2}{3}(1+\nu_0)E_{\rm ref}J^{-1/3},\ \text{for State 0}, \tag{51}$$

$$G_0 = \frac{1}{3}E_{\rm ref}J^{-1/3},\ \text{for State 0}. \tag{52}$$

Eq. (50) with $\Delta\mu = 0$ is identical to the one derived by Bouklas and Huang (2012) while when $\nu_0 = 1/2$ with $\Delta J = 0$, $E_0 = E_{\rm ref}J^{-1/3}$ of Eq. (51) is the well-known relation (Boyce and Arruda, 2001). Further, Eq. (50) shows that ν_0 in a transient

state caused by solvent migration can be estimated by taking the value of $\Delta\mu/(\upsilon\Delta\varepsilon_1)$ between $-(1/3)\,E_{\rm ref}J^{-1/3}$ and 0 in Eq. (35). In addition, as discussed in Section 4.3, G_0 is independent of $\Delta\mu = 0$ and $\Delta J = 0$.

For State I (i.e., equilibrium swelling under uniaxial loading), the explicit expressions of Eqs. (43) and (44) are also simply derived using Eq. (49), i.e.,

$$\nu_{\rm I} = \begin{cases} \frac{1}{2} - \frac{J\lambda^{-1}}{2}\left\{1 + \frac{3kT}{E_{\rm ref}\upsilon}\left(\frac{1}{J-1} - \frac{2\chi}{J}\right)\right\}^{-1}, & \text{with } \Delta\mu = 0 \\ \frac{1}{2}, \quad \text{with } \Delta J = 0 \quad \rightarrow \quad \frac{\Delta\mu}{\upsilon\Delta\varepsilon_1} = -\frac{1}{3}E_{\rm ref}\lambda^{-1} \end{cases}, \text{ for State I,} \tag{53}$$

$$E_{\rm I} = \frac{1}{3}E_{\rm ref}\left\{J^{-1}\lambda^2 + (1+2\nu_{\rm I})\lambda^{-1}\right\}, \text{ for State I,} \tag{54}$$

where λ is the stretch in the loading direction Fig. 1c). It may be convenient to replace λ with $J^{1/3}\,\alpha$ (i.e., $\lambda = J^{1/3}\,\alpha$) because λ is separated into two different contributions, namely $J^{1/3}$ owing to swelling and α owing to uniaxial loading. It is obvious that $E_{\rm I}$ and $\nu_{\rm I}$ (Eqs. (53) and (54)) reduce to E_0 and ν_0 Eqs. (50) and (51) when $\alpha = 1$ (i.e., $\lambda = J^{1/3}$).

The general expressions developed in Sections 4.2–4.4 were verified here using the original FR framework. Eqs. (50)–(54) indicate that the explicit expressions are remarkably simple because in the original FR framework, most of the derivatives of $W_{\rm e}$ become zero. This implies that when a more complex form of $W_{\rm e}$ is defined as a nonlinear function of I_1, I_2 and J, it is not realistic to show the explicit expressions. It is, however, without a doubt that the general expressions play a key role in calculating and estimating the linearized properties of swollen elastomers that depend on solvent migration and the base state. For instance, Horgan (2015) reviewed numerous developments of the Gent model, which was extended by introducing the I_2 term to well reproduce the responses of soft biomaterials (Puglisi and Saccomandi, 2016; Destrade et al., 2017). In Section 5, as analytical examples, an extended Gent model is examined to elucidate the interactions of limiting chain extensibility and the I_2 term.

5. Analytical examples

5.1. An extended Gent model with the I_2 term

To demonstrate the usefulness of the general expression for the linearized properties of swollen elastomers (Section 4), instead of the NH model, we employ the Gent model extended by the I_2 term, which is expressed as (Horgan, 2015; Puglisi and Saccomandi, 2016; Destrade et al., 2017)

$$W_{\rm e} = \frac{(1-c)E_{\rm ref}}{6}\left\{-J_{\rm m}\log\left(1 - \frac{I_1 - 3}{J_{\rm m}}\right) - 2\log J\right\} + \frac{cE_{\rm ref}}{2}\log\left(\frac{I_2}{3}\right). \tag{55}$$

Here, $J_{\rm m}$ is a material constant to describe the limiting chain extensibility (Horgan and Saccomandi, 2002; Okumura and Chester, 2018), and c = 0–1 is the ratio of the contributions of the original Gent model and the added I_2 term. If $c = 0$, Eq. (55) is reduced to the original Gent model, while as c increases the contribution of the I_2 term increases. The necessity of the I_2 term in the elastic strain energy has been historically discussed and is not discussed here (e.g., Treloar, 1975). It is noted that Eq. (55) has the ability to well reproduce the responses of soft biomaterials (Puglisi and Saccomandi, 2016; Destrade et al., 2017). The present study investigates the effect of a simple logarithmic version as the I_2 term.

The extended Gent model (Eq. (55)) is a nonlinear function that includes all the independent terms with respect to the three strain-invariants. Eqs. (15)–(20) indicate $k^{(2)} = k^{(4)} = k^{(5)} = 0$ but $k^{(1)} \neq k^{(3)} \neq k^{(6)} \neq 0$. The specific forms of $k^{(n)}$ and D_i (Eq. (27)) are shown in Appendix B. The calculations using $k^{(n)}$ and D_i allow us to estimate the Young's modulus and Poisson's ratio including the effects of solvent migration and the base state (Section 4). The interactions of limiting chain extensibility and the I_2 term (i.e., $J_{\rm m}$ and I_2 via c) are also investigated.

In Sections 5.2 and 5.3, States 0 and I are analyzed as analytical examples. For simplicity, the non-dimensional Young's modulus, $E_{\rm ref}\,\upsilon\,/(3kT)$ (Bouklas and Huang, 2012; Okumura et al., 2016), is fixed as $E_{\rm ref}\,\upsilon\,/(3kT) = 0.0001$, whereas $J_{\rm m}$, c and χ are parameterized as $J_{\rm m} = 10$, 100 and ∞, $c = 0$, 1/3, 2/3 and 0.95, and $\chi = 0$–1.2. In the case of $J_{\rm m} = \infty$, the original Gent model is reduced to the NH model. In that case Eq. (55) is reduced to the NH model extended by the I_2 term. Moreover, if $c = 0$ is additionally imposed, Eq. (55) is just the NH model (Eq. (47)).

5.2. Case of State 0 (equilibrium free swelling)

When the base state is prescribed by State 0, the volume swelling ratio, J, for equilibrium free swelling ($s_i = 0$ and $\mu = 0$) is calculated from Eqs. (4) and (5). Fig. 2 plots J as a function of the interaction parameter, χ. Fig. 2 shows the responses for the different values of $J_{\rm m} = 10$, 100 and ∞, while in the individual panels the effect of the I_2 term is parameterized by $c = 0$, 1/3, 2/3 and 0.95. According to Okumura and Chester (2018), the ultimate value of J is predicted to be $J_{\rm ult} = (J_{\rm m}/3 + 1)^{3/2}$; the values of $J_{\rm ult}$ are also plotted in the figure's panels.

Fig. 2 shows that if $\chi > 0.5$ (i.e., for a poor solvent), the effects of limiting chain extensibility and the I_2 term are negligible. This tendency is characteristic of the FR framework and the relatively small value of $E_{\rm ref}\,\upsilon\,/(3kT)$ (Okumura et al., 2016). Remarkably, the effect appears for $\chi < 0.5$ (i.e., for a good solvent). Fig. 2a shows that as the contribution of the I_2 term increases (i.e., c increases), J increases. The I_2 term is found to decrease the repulsive force against swelling. Next,

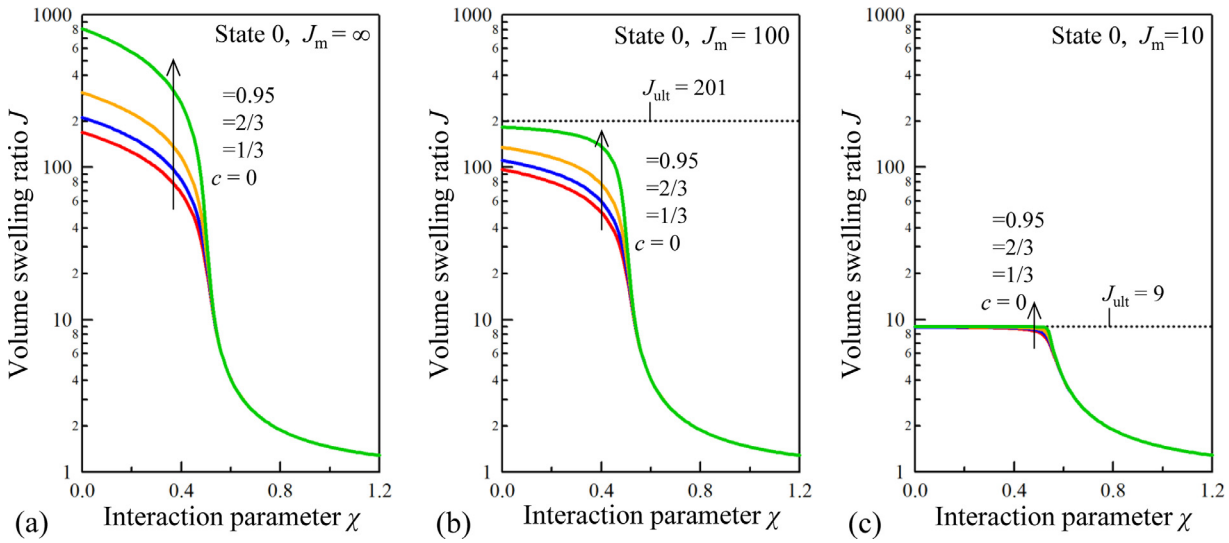

Fig. 2. Volume swelling ratio J at equilibrium free swelling (State 0) as a function of the interaction parameter χ for $E_{ref}\,\upsilon\,/(3kT)$=0.0001 with (a) $J_m = \infty$, (b) J_m =100 and (c) J_m =10, which are obtained from the fundamental equations of Eqs. (4) and (5). To investigate the effects of limiting chain extensibility and the I_2 term in the extended Gent model, J_m, c and χ are parameterized as J_m =10, 100 and ∞, c = 0, 1/3, 2/3 and 0.95, and χ = 0–1.2. The ultimate value of J is given as $J_{ult} = (J_m / 3 + 1)^{3/2}$, which depends only on J_m and is independent of the additive I_2 term (Okumura and Chester, 2018).

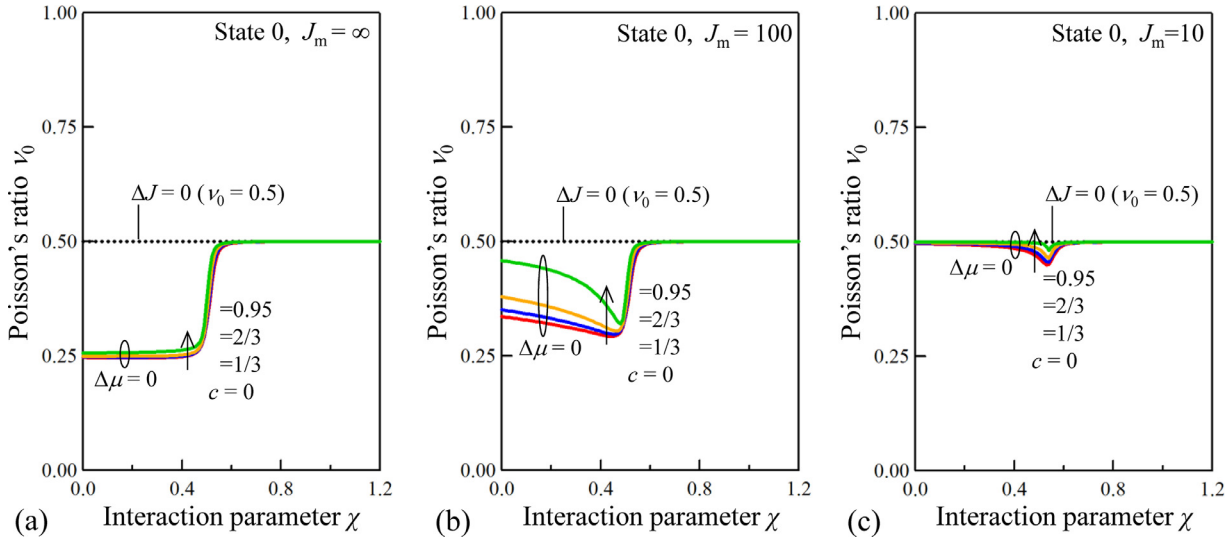

Fig. 3. Poisson's ratio ν_0 at equilibrium free swelling (State 0) as a function of the interaction parameter χ for $E_{ref}\,\upsilon\,/(3kT)$=0.0001 with (a) $J_m = \infty$, (b) J_m =100 and (c) J_m =10, which are predicted from the general expression of Eq. (36). The swelling effects caused by solvent migration gradually vanish as J_m decreases from ∞ to 10, i.e., as J approaches J_{ult}. The increase of c accelerates this tendency by causing J to increase.

Figs. 2b,c show that the decrease of J_m results in the decrease of J_{ult}. As a result, the effect of the I_2 term is gradually reduced as J_m decreases. Fig. 2c shows that the effect of the I_2 term is essentially negligible because the small value of J_m does not allow a value of J that is larger than J_{ult} for $\chi < 0.5$.

Figs. 3 and 4 show the Poisson's ratio, ν_0, and the Young's modulus, E_0, for equilibrium free swelling, respectively, that are predicted from the general expressions developed in Section 4 (Eqs. (35) and (36)). As described below, these figures successfully elucidate the characteristic behaviors of swollen elastomers that cannot be discerned from Fig. 2.

First, Fig. 3a shows that the contribution of the I_2 term is negligible for ν_0 in the case of $J_m = \infty$, i.e., $\nu_0 = 0.5$ for $\Delta J = 0$ and $\nu_0 \approx 0.25$ for $\Delta\mu = 0$, regardless of the change in c. This result indicates that under a transient state of solvent migration, ν_0 can take on a value from 0.25 to 0.5. It is interesting to compare Fig. 3a-c because the effect of limiting chain extensibility, which appears for $\chi < 0.5$ in Fig. 3b,c, increases ν_0 with $\Delta\mu = 0$ from 0.25 to 0.5. The remarkable increases occur as J approaches the ultimate value of J_{ult} (see Fig. 2). Consequently, the range of ν_0 in a transient state of solvent

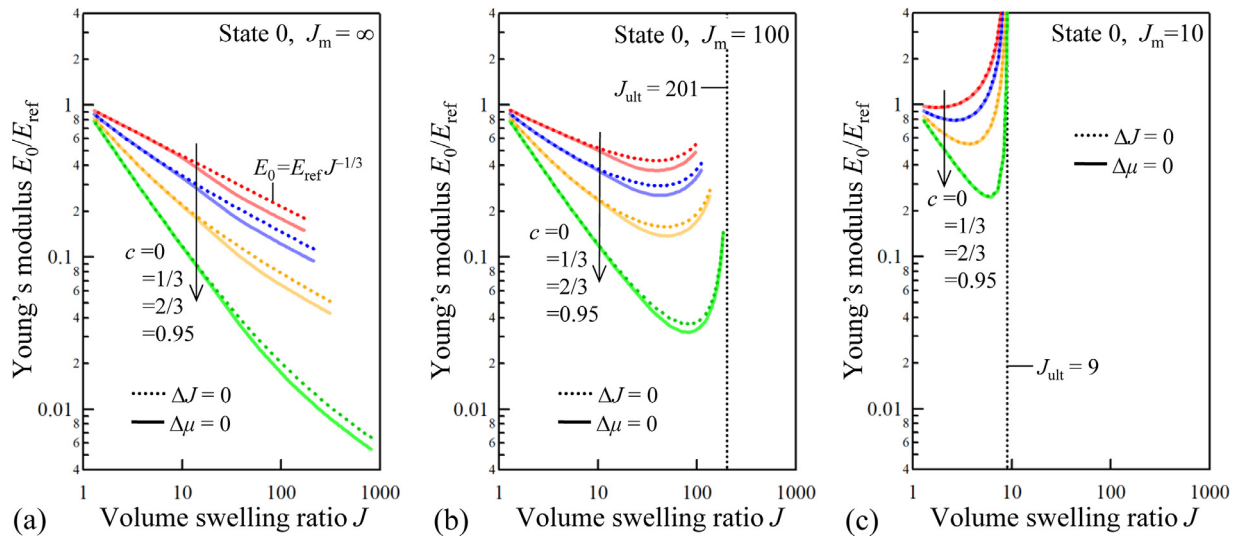

Fig. 4. Young's modulus E_0 at equilibrium free swelling (State 0) as a function of the volume swelling ratio J for $E_{ref}\,\upsilon\,/(3kT)$=0.0001 with (a) $J_m = \infty$, (b) J_m =100 and (c) J_m =10, which are predicted from the general expression of Eqs. (35) and (36). As χ decreases from 1.2 to 0, J increases monotonically. The I_2 term contributes to the additional decrease of E_0; meanwhile, limiting chain extensibility causes this dramatic increase of E_0 as J approaches J_{ult}. In contrast, the swelling effects caused by solvent migration are comparatively small.

migration becomes smaller as the contribution of the I_2 term becomes larger (i.e., c increases from 0 to 1). Fig. 3c shows that when J comes sufficiently close to J_{ult}, $\nu_0 \approx 0.5$ regardless of the values of $\Delta\mu$ and ΔJ. This surprising behavior can be understood by considering that the extreme situation of $J \approx J_{ult}$ does not allow an additional increase of J even with $\Delta\mu = 0$. It is found that the swelling effects caused by solvent migration gradually vanish as J approaches J_{ult}.

Fig. 4 shows the Young's modulus, E_0, as a function of the volume swelling ratio, J. In these figures, J increases from about 1 to a larger value because the value of χ is parameterized from 1.2 to 0. Fig. 4a demonstrates that the combination of $J_m = \infty$, $c = 0$ and $\Delta J = =0$ results in $E_0 = E_{ref} J^{-1/3}$ (Eqs. (50) and (51)). The increase of the contribution of the I_2 term is found to accelerate the decrease of E_0 as J increases. In contrast, the comparison of the responses with $\Delta\mu = 0$ and $\Delta J = 0$ shows that the swelling effects caused by solvent migration are comparatively smaller. The data in Fig. 4b,c are focused on understanding the interactions between J_m and c. The approach of J to J_{ult} causes an increase of E_0 to infinity because of the effect of limiting chain extensibility (Okumura and Chester, 2018). It is found that although the I_2 term contributes to the additional decrease of E_0 as J increases, limiting chain extensibility is what causes the dramatic increase of E_0 as J approaches the ultimate value. The individual profiles depicted in Fig. 4 are caused by a combination of the two effects owing to J_m and c.

5.3. Case of State I (equilibrium swelling under uniaxial loading)

Fig. 5 shows the stress, s, and volume swelling ratio, J, as a function of the stretch, λ, at equilibrium swelling under uniaxial loading (State I), which are calculated from Eqs. (4) and (5). Okumura and Chester (2018) reported that limiting chain extensibility contributes to providing the limit values of the stretch and volume swelling ratio under uniaxial loading, which are plotted as λ_{lim} and J_{lim}, respectively (Fig. 5b,d). These values are given as $\lambda_{lim} = (J_m + 3)^{1/2}$ and $J_{lim} =(\lambda\ /2)(J_m + 3 - \lambda^2)$, which depend only on J_m and are independent of the additive I_2 term because of the form of Eq. (55). Additionally, in Fig. 5a,b, the responses with $J = 1$ (i.e., $\mu = -\infty$) are also plotted for comparison.

Fig. 5a,c shows that for $J_m = \infty$, the stress and volume swelling ratio increase monotonically as λ increases. The increase of c has the tendency to decrease s and increase J. The decrease in s is the reason that the I_2 term is used to well reproduce the experimentally measured stress–stretch curves of elastomers (Puglisi and Saccomandi, 2016; Destrade et al., 2017), while the increase in J latter is the swelling contribution resulting from the I_2 term (see Fig. 2 for State 0). Fig. 5b,d shows the interactions between c and J_m, i.e., the I_2 term and limiting chain extensibility. It is found that the increase of c allows J to approach J_{lim} (Fig. 5d) and that regardless of the value of c, s increases steeply with an infinitely large gradient as λ approaches to λ_{lim} (Fig. 5c). In this singular situation, J decreases again to 1 (Fig. 5d), i.e., deswelling occurs even under tension (Okumura and Chester, 2018). If further discussions are to be provided via the analysis of the Young's modulus and Poisson's ratio, it is worthwhile understanding the characteristic behavior of swollen elastomers predicted by the extended Gent model.

Fig. 6a,b shows the Poisson ratio, ν_I, as a function of the stretch, λ, as predicted from the general expressions (Eqs. (43) and (44)). For $J_m = \infty$, Fig. 6a indicates that ν_I with $\Delta\mu = 0$ is not sensitive to changes of λ under tension and compression

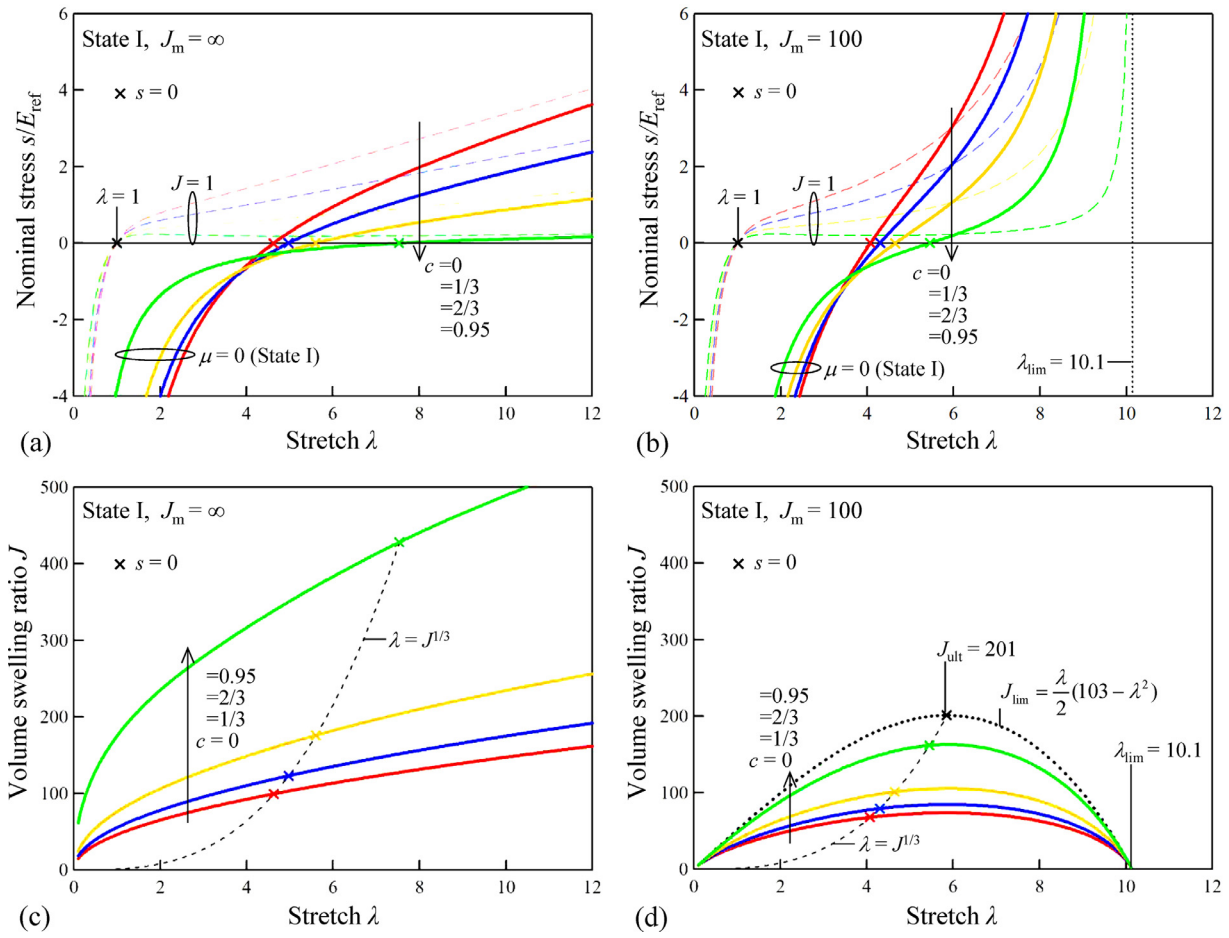

Fig. 5. Stress s and volume swelling ratio J as a function of stretch λ at equilibrium swelling under uniaxial loading (State I) for $E_{ref}\,\upsilon\,/(3kT) = 0.0001$ and χ =0.3, which are obtained from the fundamental equations of Eqs. (4) and (5). (a) s–λ for $J_m = \infty$, (b) s–λ for $J_m = 100$, (c) J–λ for $J_m = \infty$, and (d) J–λ for J_m =100. According to Okumura and Chester (2018), the limit values are given as $\lambda_{lim} = (J_m + 3)^{1/2}$ and $J_{lim} = (\lambda\,/2)(J_m + 3 - \lambda^2)$, which depend only on J_m and are independent of the additive I_2 term. When λ approaches λ_{lim}, deswelling can occur even under tension. In Fig. 5a,b, the response with the constant $J = 1$ (i.e., $\mu = -\infty$) is also plotted for comparison.

and that the effect of solvent migration has a monotonic effect on the change of ν_I in the range from 0.25–0.5. In contrast, a finite value of J_m, i.e., the effect of limiting chain extensibility, causes an unbelievable change in Poisson's ratio (Fig. 6b). Although at $s = 0$, ν_I has a finite value between 0.25 and 0.5 (also see Fig. 3b), the value of ν_I with $\Delta\mu = 0$ increases dramatically beyond 1 when λ approaches λ_{lim} under tension. Further, under compression, the value of ν_I decreases to 0 as λ decreases to a limit value under compression (the value is almost 0). Fig. 6a,b demonstrates that when the value of J_m is finite, the value of ν_I characteristically varies significantly as a result of the interactions of solvent migration and limiting chain extensibility. In this case, the contribution of the I_2 term is found to be qualitative in a secondary manner.

By focusing on the variations in the value of ν_I (Fig. 6b), the mechanism can be explained as a specific contribution caused by deswelling, as described below. First, when λ approaches the limit values under tension and compression, deswelling occurs with $\Delta\mu = 0$ (Fig. 5d). The volume swelling ratio J attempts to decrease to 1, i.e., approaches the perfectly dry state (Okumura and Chester, 2018). In an extreme state under tension, a further tensile stretch induces additional deswelling, i.e., J gradually approaches 1 (but not below 1) so that the value of ν_I is above 0.5 and steadily increases with an infinite gradient. Conversely, deswelling induces ν_I to gradually decrease to 0 under compression.

Moreover, Fig. 6c,d show the Young's modulus, E_I, as a function of the stretch, λ. The value of E_I decreases as c increases, which is caused by the contribution of the I_2 term. In contrast, the contribution caused by limiting chain extensibility shows that the degree of the increase of E_I is accelerated as λ increases under tension, or decreases under compression. This is due to the finite value of J_m, which yields the limit values of λ under tension and compression. When the linearized properties of swollen elastomers are predicted for the extended FR framework, the general expression developed in Section 4 successfully provides the individual values that include the interactions of solvent migration and the nonlinearity of the elastic free energy.

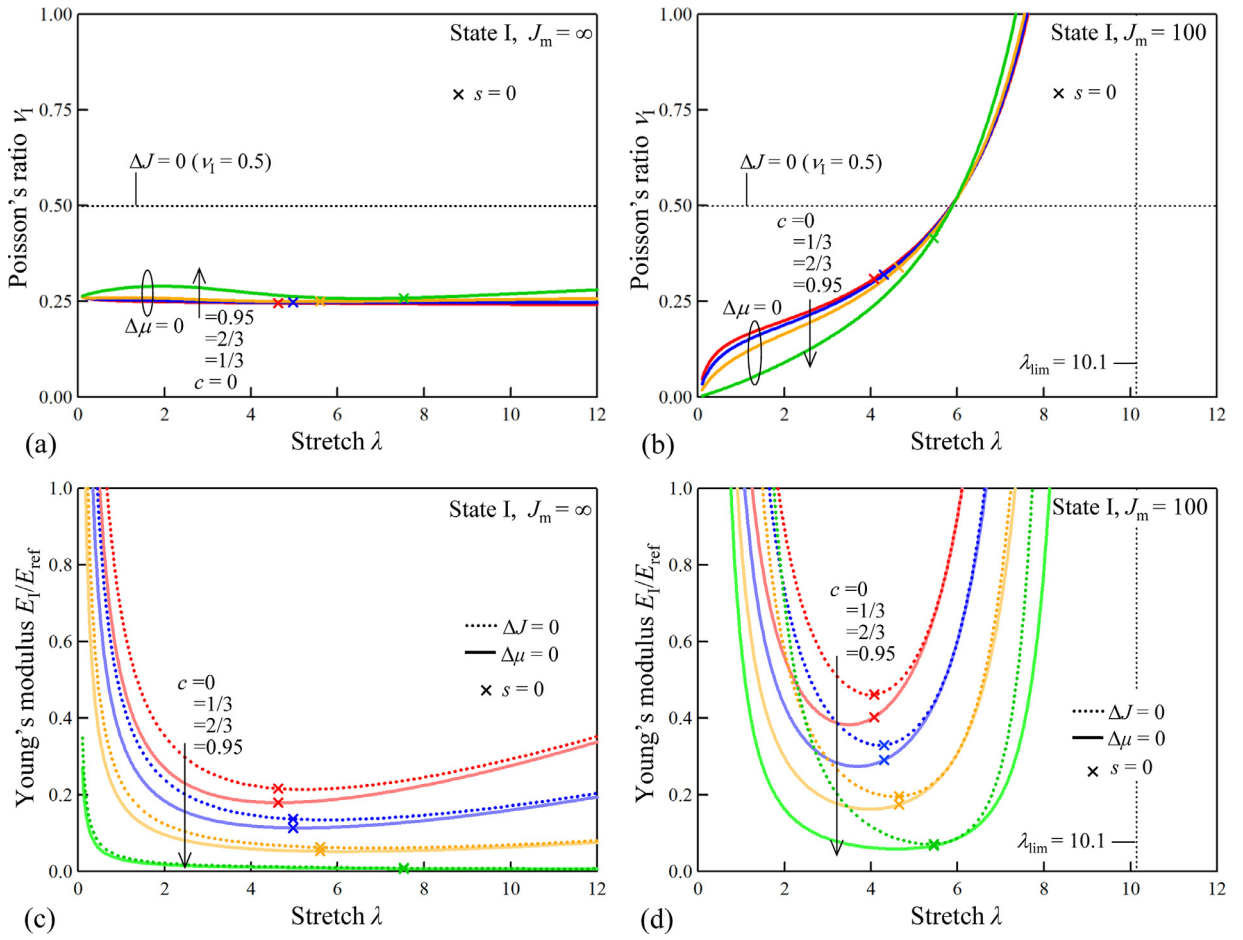

Fig. 6. Poisson's ratio ν_1 and Young's modulus E_1 as a function of stretch λ at equilibrium swelling under uniaxial loading (State I) for $E_{ref}\ \upsilon\ /(3kT) = 0.0001$ and $\chi = 0.3$, as predicted from the general expression of Eqs. (43) and (44). (a) ν_1–λ for $J_m = \infty$, (b) ν_1–λ for $J_m = 100$, (c) E_1–λ for $J_m = \infty$, and (d) E_1–λ for $J_m = 100$. The predicted values are highly variable and are a result of the interactions of solvent migration, limiting chain extensibility and the I_2 term effect, i.e., the combination of ΔJ, $\Delta\mu$, J_m and c.

6. Conclusions

In the present study, we developed the general expression for the linearized properties of swollen elastomers undergoing large deformations. The FFR hypothesis and FR framework were assumed to describe the free energy function of swollen elastomers. However, no particular form was assumed to be the strain-energy function, which was instead assumed only to be a function of a set of strain-invariants. A linearization procedure was used to obtain the general expression of the Young's modulus and Poisson's ratio from an arbitrary base state. A characteristic term in the derived expression has the ability to describe a transient state between the extreme conditions prescribed by the two distinct conditions, $\Delta J = 0$ and $\Delta\mu = 0$. The verification was performed by estimating the shear modulus and considering the original Flory–Rehner framework. In addition, to show the usefulness, an extended Gent model was examined to elucidate the interactions between limiting chain extensibility and the second strain-invariant with the swelling effects caused by solvent migration.

The developed analytical procedure should provide a simple but comprehensive understanding of the response of swollen elastomers. Although the present study focused on one of the extended Gent models as an example, the general expression developed here allows more advanced strain-energy functions to be systematically analyzed. Recently, Horgan (2015) reviewed the numerous developments, extensions and widespread applications not only in rubber elasticity but also in the area of biomechanics of soft biomaterials. As reported by Destrade et al. (2009), soft biomaterials, such as soft tissues, arteries, dura matters, and muscles, need an extremely small value of J_m. The range for soft biomaterials is about $0.1 < J_m < 10$, while the range for rubbers is $20 < J_m < 200$ (Destrade et al., 2009). This discrepancy may be resolved as a characteristic response of swollen elastomers because soft biomaterials are often modeled as swollen elastomers. The effects and interactions discussed in the present study and in Okumura and Chester (2018) are expected to play a key role in demonstrating the mechanics of soft biomaterials.

Finally, readers are reminded that the linearized properties derived here are only valid for small perturbations applied to a given base state and not for large deformations from the dry state. We envision this would be useful for experimentalists as well as those interested in instabilities in swollen elastomers where the linearized properties are essential (e.g., Liu et al., 2011). It must be very important to compare the predictions with experiments. The comparison is not simple because the swelling process depends on many external stimuli (e.g., Zheng et al., 2018). Although the present study has just focused on developing a simple analytical procedure to estimate and understand the constitutive behavior based on the FFR hypothesis, there is no doubt that developments of the experimental procedures for measurements are also needed to quantitatively compare and validate the developed theories, such as the extended Gent model.

Declaration of Competing Interest

The authors declare that they have no known competing financial interests or personal relationships that could have appeared to influence the work reported in this paper.

Acknowledgments

This work was partially supported by the Japan Society for the Promotion of Science (JSPS) under a Grant-in-Aid for Scientific Research (A) (JP19H00739) and the US National Science Foundation (CMMI-1463121 and CMMI-1751520).

Appendix A. Derivation of Eq. (13)

When the small perturbations of the strain and stress are defined in Eqs. (11) and (12), i.e., $\Delta\varepsilon_i = \Delta\lambda_i/\lambda_i$ and $\Delta\sigma_i = (\lambda_i/J)\,\Delta s_i$ (no sum on i), the matrix form between $\Delta\sigma_i$ and $\Delta\varepsilon_i$ is derived as Eq. (13). In Eq. (13), the components of S_{ij} and D_i are expressed as

$$\begin{cases} S_{ij} = N_{ik}H_{kl}L_{lj} + M_{ij} \\ D_i = N_{ik}h_k \end{cases}, \tag{A.1}$$

where

$$N_{ij} = \begin{bmatrix} \lambda_1^4 & \lambda_1^2 & 1 \\ \lambda_2^4 & \lambda_2^2 & 1 \\ \lambda_3^4 & \lambda_3^2 & 1 \end{bmatrix}, \tag{A.2}$$

$$H_{ij} = \begin{bmatrix} \frac{-2}{J}\frac{\partial^2 W_e}{\partial I_1 \partial I_2} & \frac{-2}{J}\frac{\partial^2 W_e}{\partial I_2^2} & \frac{-2}{J}\frac{\partial^2 W_e}{\partial I_2 \partial J} \\ \frac{2}{J}\left(\frac{\partial^2 W_e}{\partial I_1^2} + \frac{\partial^2 W_e}{\partial I_2^2} + I_1\frac{\partial^2 W_e}{\partial I_1 \partial I_2}\right) & \frac{2}{J}\left(I_1\frac{\partial^2 W_e}{\partial I_2^2} + \frac{\partial^2 W_e}{\partial I_1 \partial I_2}\right) & \frac{2}{J}\left(I_1\frac{\partial^2 W_e}{\partial I_2 \partial J} + \frac{\partial^2 W_e}{\partial J \partial I_1}\right) \\ \frac{\partial^2 W_e}{\partial J \partial I_1} & \frac{\partial^2 W_e}{\partial I_2 \partial J} & \frac{\partial^2 W_e}{\partial I_2^2} + \frac{1}{J}\left(\frac{\partial W_e}{\partial J} - \Pi\right) \end{bmatrix}, \tag{A.3}$$

$$L_{ij} = \begin{bmatrix} 2\lambda_1^2 & 2\lambda_2^2 & 2\lambda_3^2 \\ 2\lambda_1^2(I_1 - \lambda_1^2) & 2\lambda_2^2(I_1 - \lambda_2^2) & 2\lambda_3^2(I_1 - \lambda_3^2) \\ J & J & J \end{bmatrix}, \tag{A.4}$$

$$M_{ij} = J\frac{\partial^2 W_m}{\partial J^2}\begin{bmatrix} 1 & 1 & 1 \\ 1 & 1 & 1 \\ 1 & 1 & 1 \end{bmatrix}, \tag{A.5}$$

$$h_i = \begin{Bmatrix} -\frac{6}{J}\frac{\partial W_e}{\partial I_2} \\ \frac{2}{J}\left(\frac{\partial W_e}{\partial I_1} + I_1\frac{\partial W_e}{\partial I_2}\right) \\ -\frac{\partial W_e}{\partial J} + \Pi \end{Bmatrix}. \tag{A.6}$$

Although Eq. (A.1) does not clearly show the symmetry of $S_{ij} = S_{ji}$, a different expression for S_{ij} is shown in Eq. (14) using $k^{(n)}$ and $S_{ij}^{(n)}$ ($n = =1, 2, 3,\ldots, 6$) (Eqs. (15)–(26)). Since the individual matrices of $S_{ij}^{(n)}$ are symmetric, S_{ij} is also symmetric. This symmetry yields the reciprocal relations, which reduce the number of distinct Poisson's ratios from six to only three (e.g., Vannucci, 2018). Thus, Eqs. (13) and (29) have the ability to provide the three Young's moduli and three Poisson's ratios depending on an arbitrary base state.

Appendix B. Derivation of $k^{(n)}$ and D_i for Eq. (55)

When the extended Gent model Eq. (55) is used as the elastic strain energy in the FR framework, then $k^{(2)} = k^{(4)} = k^{(5)} = 0$; however, $k^{(1)} \neq k^{(3)} \neq k^{(6)} \neq 0$ in Eqs. (15)–(20). The non-zero variables are given as

$$k^{(1)} = \frac{2E_{ref}}{J}\left\{\frac{c}{I_2} + \frac{(1-c)J_m}{3(J_m - I_1 + 3)^2}\right\}, \tag{B.1}$$

$$k^{(3)} = -\frac{2cE_{\mathrm{ref}}}{I_2^2 J}, \tag{B.2}$$

$$k^{(6)} = \frac{E_{\mathrm{ref}}}{3J}\left\{(1-c)\left(1-\frac{J_{\mathrm{m}}\lambda_3^2}{J_{\mathrm{m}}-I_1+3}\right)-\frac{3c\lambda_3^2(I_1-\lambda_3^2)}{I_2}+\frac{3kT}{E_{\mathrm{ref}}\upsilon}\left(\frac{1}{J-1}-\frac{2\chi}{J}\right)\right\}, \tag{B.3}$$

where $k^{(6)}$ is obtained using Eq. (6) to replace Π with terms based on W_{e} because Eq. (6) can be used in the case of $s_3 = 0$, i.e., in States 0, I and II.

Eqs. (B.1)–(B.3) give the specific form of S_{ij} (Eq. (14)) as

$$S_{ij} = k^{(1)}S_{ij}^{(1)} + k^{(3)}S_{ij}^{(3)} + k^{(6)}S_{ij}^{(6)}, \tag{B.4}$$

where $S_{ij}^{(1)}$, $S_{ij}^{(3)}$ and $S_{ij}^{(6)}$ are shown in Eqs. (21), (23) and (26), respectively. Further, Eq. (27) gives the specific form of D_i, and is expressed as

$$D_i = \frac{E_{\mathrm{ref}}}{3J}\left[\frac{(1-c)(\lambda_i^2+\lambda_3^2)J_{\mathrm{m}}}{J_{\mathrm{m}}-I_1+3}+\frac{3c}{I_2}\left\{\lambda_i^2(I_1-3\lambda_i^2)+\lambda_3^2(I_1-\lambda_3^2)\right\}\right], \tag{B.5}$$

which is derived using Eq. (6) in the same way as Eq. (B.3). It is obvious that if $J_{\mathrm{m}} = \infty$ and $c = 0$, Eqs. (B.1)–(B.5) are reduced to the equations for the original FR framework, i.e., $k^{(1)} = k^{(3)} = 0$ and $S_{ij} = k^{(6)}$ ($i = =1, 2, 3$, $j = =1, 2, 3$) (cf. Eq. (49)).

References

Abaqus 6.14 User Documentation, 2014, Dassault systems simulia coorporation.

Beatty, M.F., Stalnaker, D.O., 1986. The Poisson function of finite elasticity. J. Appl. Mech. 53, 807–813.

Bitoh, Y., Urayama, K., Takigawa, T., Ito, K., 2011. Biaxial strain testing of extremely soft polymer gels. Soft Matter 7, 2632–2638.

Bouklas, N., Huang, R., 2012. Swelling kinetics of polymer gels: comparison of linear and nonlinear theories. Soft Matter 8, 8194–8203.

Bouklas, N., Landis, C.M., Huang, R., 2015. A nonlinear, transient finite element method for coupled solvent diffusion and large deformation of hydrogels. J. Mech. Phys. Solids 79, 21–43.

Boyce, M.C., Arruda, E.M., 2001. Swelling and mechanical stretching of elastomeric materials. Math. Mech. Solids 6, 641–659.

Chester, S.A., Anand, L., 2010. A coupled theory of fluid permeation and large deformations for elastomeric materials. J. Mech. Phys. Solids 58, 1879–1906.

Chester, S.A., Anand, L., 2011. A thermo-mechanically coupled theory for fluid permeation in elastomeric materials: application to thermally responsive gels. J. Mech. Phys. Solids 59, 1978–2006.

Davidson, J.D., Goulbourne, N.C., 2013. A nonaffine network model for elastomers undergoing finite deformations. J. Mech. Phys. Solids 61, 1784–1797.

Destrade, M., Annaidh, A.N., Coman, C.D., 2009. Bending instabilities of soft biological tissues. Int. J. Solids Struct. 46, 4322–4330.

Destrade, M., Saccomandi, G., Sgura, I., 2017. Methodical fitting for mathematical models of rubber-like materials. Proc. R. Soc. A 473, 20160811.

Doi, M., 2013. Soft Matter Physics. Oxford University Press, Oxford, UK.

Drozdov, A.D., Christiansen, J.deC., 2013. Stress–strain relations for hydrogels under multiaxial deformation. Int. J. Solids Struct. 50, 3570–3585.

Flory, P.J., 1953. Principles of Polymer Chemistry. Cornell University Press, Ithaca, NY.

Flory, P.J., Rehner, J., 1943. Statistical mechanics of cross-linked polymer networks II. Swelling. J. Chem. Phys. 11, 521–526.

Frenkel, J., 1940. A theory of elasticity, viscosity and swelling in polymeric rubber-like substances. Rubber Chem. Technol. 13, 264–274.

Holzapfel, G.A., 2000. Nonlinear Solid Mechanics, A Continuum Approach for Engineering. John Wiley & Sons Ltd, England.

Hong, W., Liu, Z.S., Suo, Z., 2009. Inhomogeneous swelling of a gel in equilibrium with a solvent and mechanical load. Int. J. Solids Struct. 46, 3282–3289.

Hong, W., Zhao, X., Zhou, J., Suo, Z., 2008. A theory of coupled diffusion and large deformation in polymeric gels. J. Mech. Phys. Solids 56, 1779–1793.

Horgan, C.O., 2015. The remarkable gent constitutive model for hyperelastic materials. Int. J. Non-Linear Mech. 68, 9–16.

Horgan, C.O., Saccomandi, G., 2002. A molecular-statistical basis for the Gent constitutive model of rubber elasticity. J. Elasticity 68, 167–176.

Kang, M.K., Huang, R., 2010a. A variational approach and finite element implementation for swelling of polymeric hydrogels under geometric constraints. J. Appl. Mech. 77, 061004.

Kang, M.K., Huang, R., 2010b. Swelling-induced surface instability of confined hydrogel layers on substrates. J. Mech. Phys. Solids 58, 1582–1598.

Li, J., Suo, Z., Vlassak, J.J., 2014. A model of ideal elastomeric gels for polyelectrolyte gels. Soft Matter 10, 2582–2590.

Liu, Z.S., Swaddiwudhipong, S., Cui, F.S., Hong, W., Suo, Z., Zhang, Y.W., 2011. Analytical solutions of polymeric gel structures under buckling and wrinkle. Int. J. Appl. Mech. 3, 235–257.

Liu, Z.S., Toh, W., Ng, T.Y., 2015. Advances in mechanics of soft materials: a review of large deformation behavior of hydrogels. Int. J. Appl. Mech. 7, 1530001.

Mao, Y., Anand, L., 2018. A theory for fracture of polymeric gels. J. Mech. Phys. Solids 115, 30–53.

McKenna, G.B., Flynn, K.M., Chen, Y., 1989. Experiments on the elasticity of dry and swollen networks: implications for the Frenkel–Flory–Rehner hypothesis. Macromolecules 22, 4507–4512.

Okumura, D., Chester, S.A., 2018. Ultimate swelling described by limiting chain extensibility of swollen elastomers. Int. J. Mech. Sci. 144, 531–539.

Okumura, D., Inagaki, T., Ohno, N., 2015. Effect of prestrains on swelling-induced buckling patterns in gel films with a square lattice of holes. Int. J. Solids Struct. 58, 288–300.

Okumura, D., Kondo, A., Ohno, N., 2016. Using two scaling exponents to describe the mechanical properties of swollen elastomers. J. Mech. Phys. Solids 90, 61–76.

Okumura, D., Kuwayama, T., Ohno, N., 2014. Effect of geometrical imperfections on swelling-induced buckling patterns in gel films with a square lattice of holes. Int. J. Solids Struct. 51, 154–163.

Okumura, D., Mizutani, M., Tanaka, H., Uchida, M., 2018. Effects of two scaling exponents on biaxial deformation and mass transport of swollen elastomers. Int. J. Mech. Sci. 146–147, 507–516.

Puglisi, G., Saccomandi, G., 2016. Multi-scale modelling of rubber-like materials and soft tissues: an appraisal. Proc. R. Soc. A 472, 20160060.

Toh, W., Ding, Z., Ng, T.Y., Liu, Z.S., 2015. Wrinkling of a polymeric gel during transient swelling. J. Appl. Mech. 82, 061004.

Treloar, L.R.G., 1975. The Physics of Rubber Elasticity, 3rd ed. Clarendon Press, Oxford.

Vannucci, P., 2018. Anisotropic Elasticity. Lecture Notes in Applied and Computational Mechanics 85. Springer, Singapore.

Zheng, S., Li, Z., Liu, Z.S., 2018. The fast homogeneous diffusion of hydrogel under different stimuli. Int. J. Mech. Sci. 137, 263–270.